

Biophysical Journal, Volume 112

Supplemental Information

Mechanistic Models Fit to Variable Temperature Calorimetric Data Provide Insights into Cooperativity

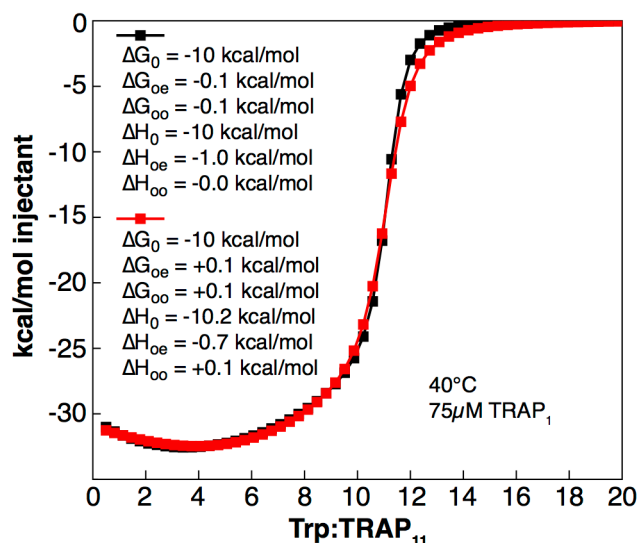
Elihu C. Ihms, Ian R. Kleckner, Paul Gollnick, and Mark P. Foster

Supporting Information for:

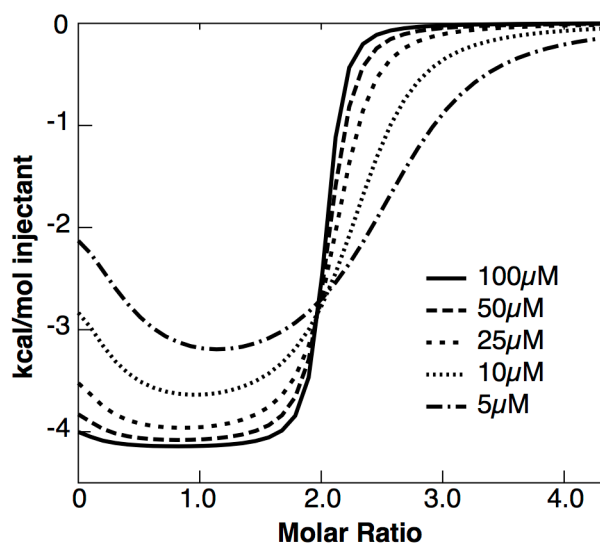
Mechanistic models fit to variable temperature calorimetric data provide insights into cooperativity

Table of Contents

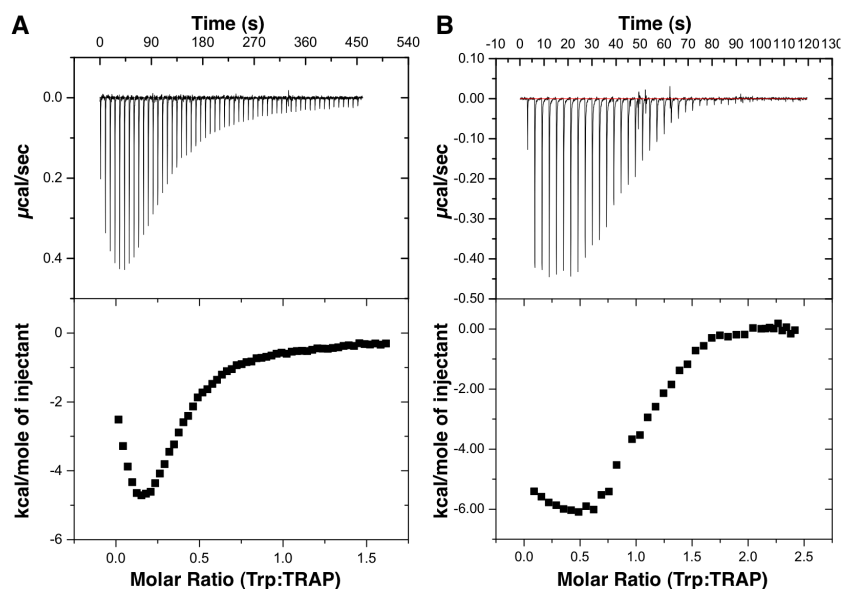
Figure S1. Similarity of individual isotherms for cooperative and uncooperative binding behavior	S2
Figure S2. Effect of C-value on discernment of different binding modes	S2
Figure S3. Example ITC isotherms of wt. <i>B. stearothermophilus</i> and <i>B. subtilis</i> TRAP	S3
Figure S4. Global fit to ITC data using phenomenological 2-mode model	S3
Table S1. Best-fit parameters for the additive cooperativity model NN-a	S4
Table S2. Best-fit parameters for the non-additive cooperativity model NN-na	S4
Figure S5. Best-fit parameters for the model NN-na	S4
Figure S6. Chi-square error surfaces for ΔG parameters model NN-na	S5
Figure S7. Chi-square error surfaces for ΔH parameters of model NN-na	S6
Figure S8. Chi-square error surfaces for ΔC_p parameters of model NN-na	S7
Figure S9. TRAP+nTrp populations for a non-cooperative (independent) NN binding model	S8
Figure S10. TRAP+nTrp populations model NN-a	S8
Figure S11. Example TRAP+Trp configurations described in the model NN-na	S9
Figure S12. Predicted populations of TRAP+Trp configurations present during 40°C ITC titration ...	S10
Figure S13. Hill equation fits to site occupancy predicted by model NN-na	S11
Figure S14. Effect of tryptophan concentration range on Hill coefficient determination.	S11



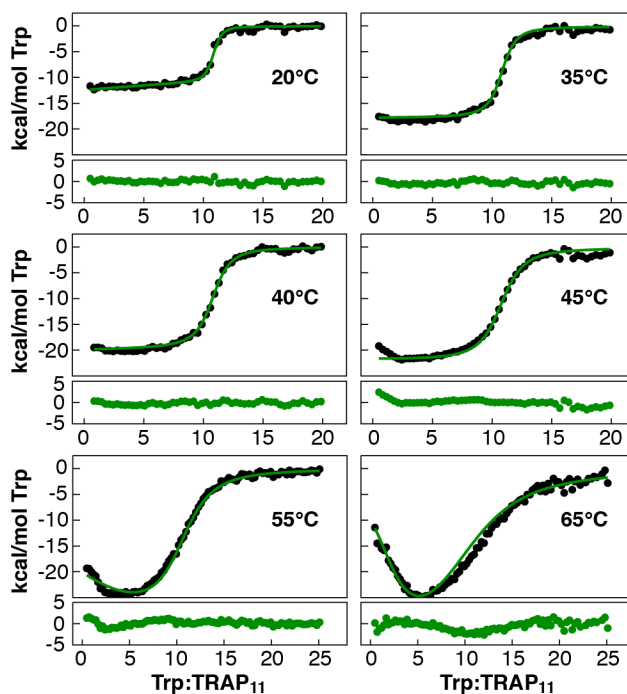
Supporting Figure 1. Similarity of predicted isotherms for cooperative and uncooperative binding behavior. Two separate predicted titration isotherms are shown, obtained from the non-additive nearest neighbor model described in the manuscript. The isotherm plotted in black is obtained under positive cooperativity conditions where binding to sites flanked by occupied neighbors is favored by 0.1 kcal/mol. The isotherm plotted in red is obtained under negative cooperativity conditions where binding next to occupied neighbors is disfavored by 0.1 kcal/mol. The similarity between the two titrations illustrates how variations in enthalpy for any single set of experimental conditions may prevent accurate determination of binding behavior.



Supporting Figure 2. Effects of C-value on ability to distinguish multiple binding modes. High C-values ($C = [\text{Macromolecule}] / K_d$) can cause the presence of multiple binding modes to be nearly undetectable. An independent two-mode binding model with one mode possessing a K_d of $5 \mu\text{M}$ and ΔH of -4 kcal/mol and a second mode possessing a K_d of $1 \mu\text{M}$ and a ΔH of -4 kcal/mol was evaluated at 5 different macromolecule concentrations. At macromolecule concentrations $> 100 \mu\text{M}$, the different binding modes become obscured, and the isotherm approaches a step function.



Supporting Figure 3. Isotherms of Trp binding to wild-type *B. stearothermophilus* and *B. subtilis* TRAP. (A) Titration of 587 μM Trp into 7.7 μM *B. stearothermophilus* wt TRAP at 25°C. (B) Titration of 890 μM Trp into 70 μM *B. subtilis* TRAP at 25°C.



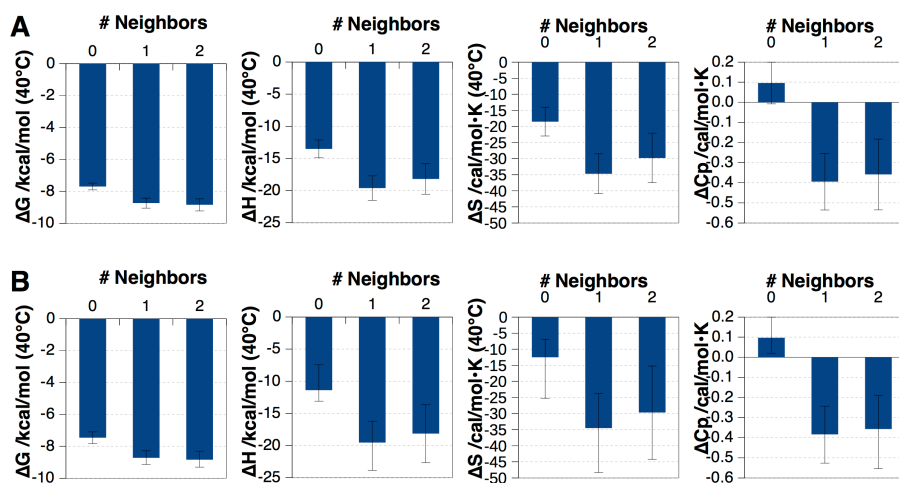
Supporting Figure 4. Global fit to experimental data using phenomenological model consisting of two independent binding modes. Integrated enthalpic heats per injection (black circles) at different temperatures are globally fit (green lines) using the model parameters $n_1 = 1.41$, $\Delta G_1 = -9.24$ kcal/mol, $\Delta H_1 = -7.50$ kcal/mol, $\Delta C_{p,1} = 0.303$ kcal/mol/K, $n_2 = 9.19$, $\Delta G_2 = -9.20$ kcal/mol, $\Delta H_2 = -20.5$ kcal/mol, and $\Delta C_{p,2} = -0.504$ kcal/mol/K. Residuals from the fit are shown below each isotherm.

NN	$\Delta G_{\text{coupling}}$		ΔG_{bind}		$\Delta H_{\text{coupling}}$		ΔH_{bind}		$\Delta C_{p,\text{coupling}}$		$\Delta C_{p,\text{bind}}$		K_d	
	low	high	low	high	low	high	low	high	low	high	low	high	low	high
0	-	-	-8.06	-7.29	-	-	-22.21	-20.10	-	-	-0.44	-0.36	2.36	8.11
1	-0.48	-0.44	-8.54	-7.73	1.30	1.76	-20.91	-18.34	0.01	0.04	-0.43	-0.33	1.09	4.02
2	-0.96	-0.87	-9.03	-8.17	2.60	3.52	-19.61	-16.58	0.02	0.07	-0.42	-0.29	0.50	2.00
	$kcal\ mol^{-1}$				$kcal\ mol^{-1}$				$kcal\ mol^{-1}\ K^{-1}$				μM	

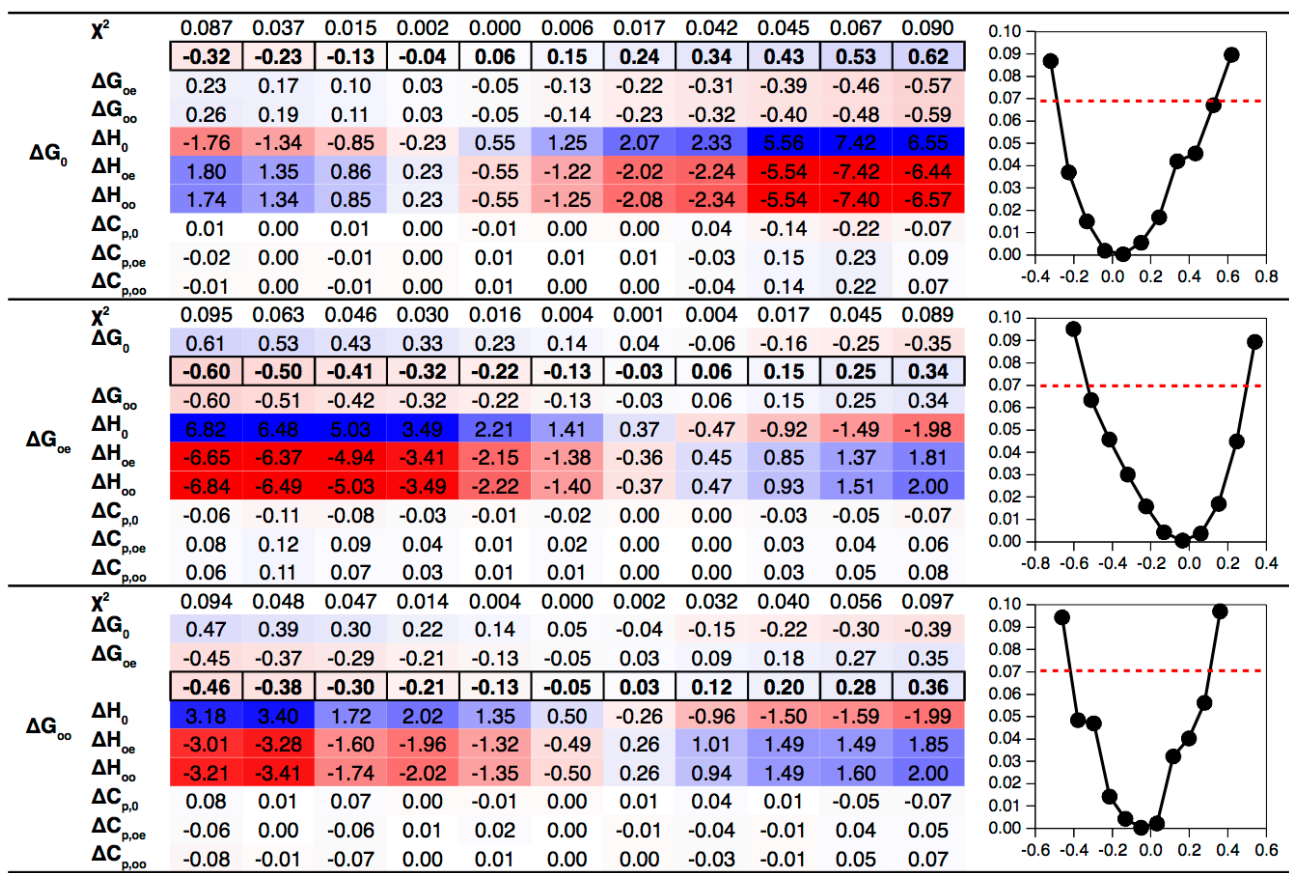
Supporting Table 1. Confidence intervals for the additive model NN-a parameters ($\pm 1SD$), obtained by a constant chi-square approach for 409 fitted datapoints. Globally-fit parameters are given at a reference temperature of 40°C (313.15 K). NN, number of occupied nearest neighbors. Fitted energy terms in grey, coupling energies for NN=2 sites are simply twice the values for NN=1; aggregate energies for other terms are obtained from the sum of ΔG_0 and coupling terms. Equilibrium constants from $\Delta G_{\text{bind}} = RT \ln K_d$ at 40°C.

NN	$\Delta G_{\text{coupling}}$		ΔG_{bind}		$\Delta H_{\text{coupling}}$		ΔH_{bind}		$\Delta C_{p,\text{coupling}}$		$\Delta C_{p,\text{bind}}$		K_d	
	low	high	low	high	low	high	low	high	low	high	low	high	low	high
0	-	-	-7.84	-7.09	-	-	-13.10	-7.40	-	-	0.00	0.17	3.38	11.23
1	-1.51	-1.07	-9.35	-8.16	-11.00	-6.52	-24.10	-13.93	-0.58	-0.36	-0.58	-0.19	0.30	2.01
2	-1.65	-1.17	-9.49	-8.26	-9.79	-5.40	-22.90	-12.81	-0.55	-0.32	-0.55	-0.14	0.24	1.72
	$kcal\ mol^{-1}$				$kcal\ mol^{-1}$				$kcal\ mol^{-1}\ K^{-1}$				μM	

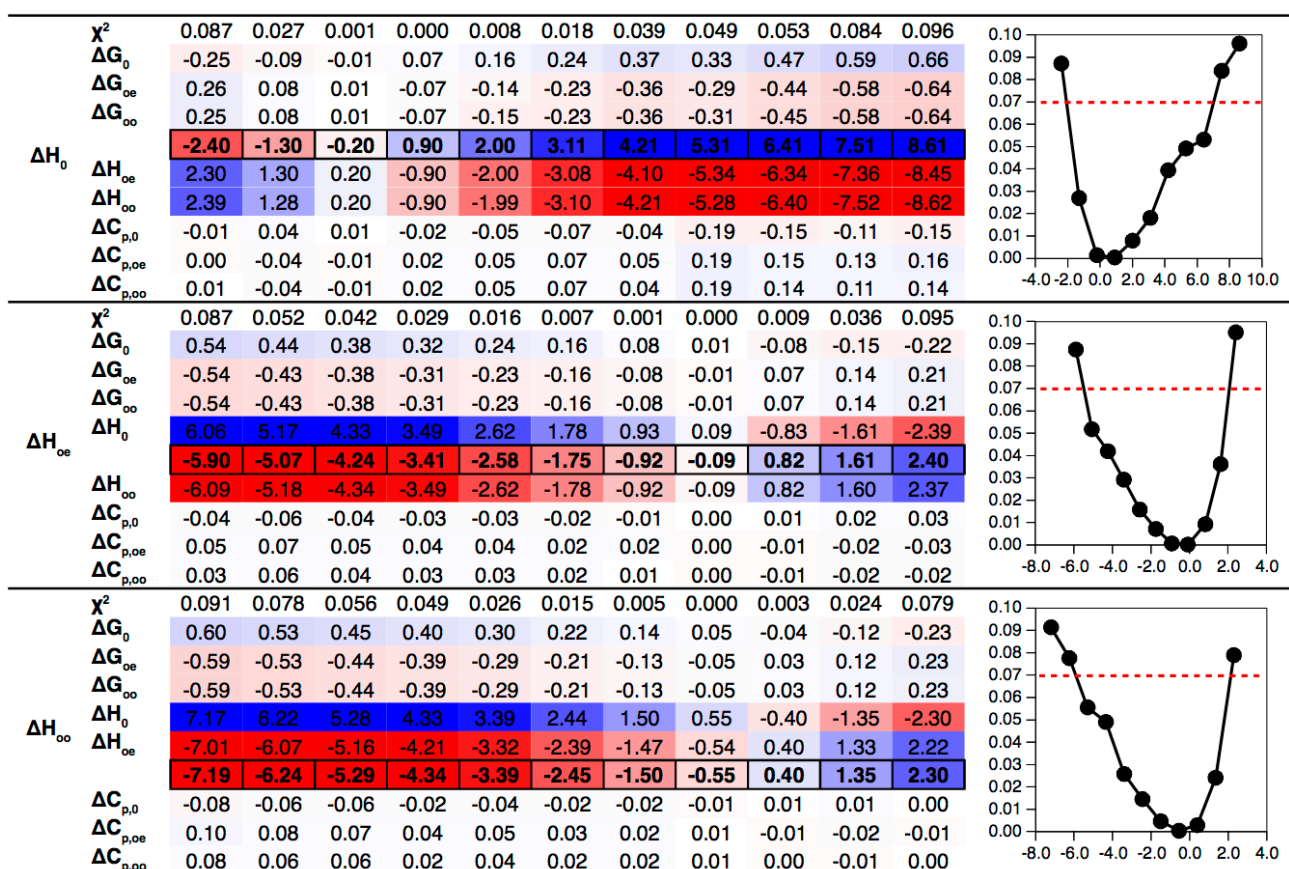
Supporting Table 2. Confidence intervals for the non-additive model NN-na parameters ($\pm 1SD$), obtained by the constant chi-square approach for 409 fitted datapoints, described in figures S6-S8. Globally-fit parameters are given at a reference temperature of 40°C (313.15 K). NN, number of occupied nearest neighbors. Fitted energy terms in grey, aggregate energies for other terms are obtained from the sum of ΔG_0 and coupling terms. Equilibrium constants from $\Delta G_{\text{bind}} = RT \ln K_d$ at 40°C.



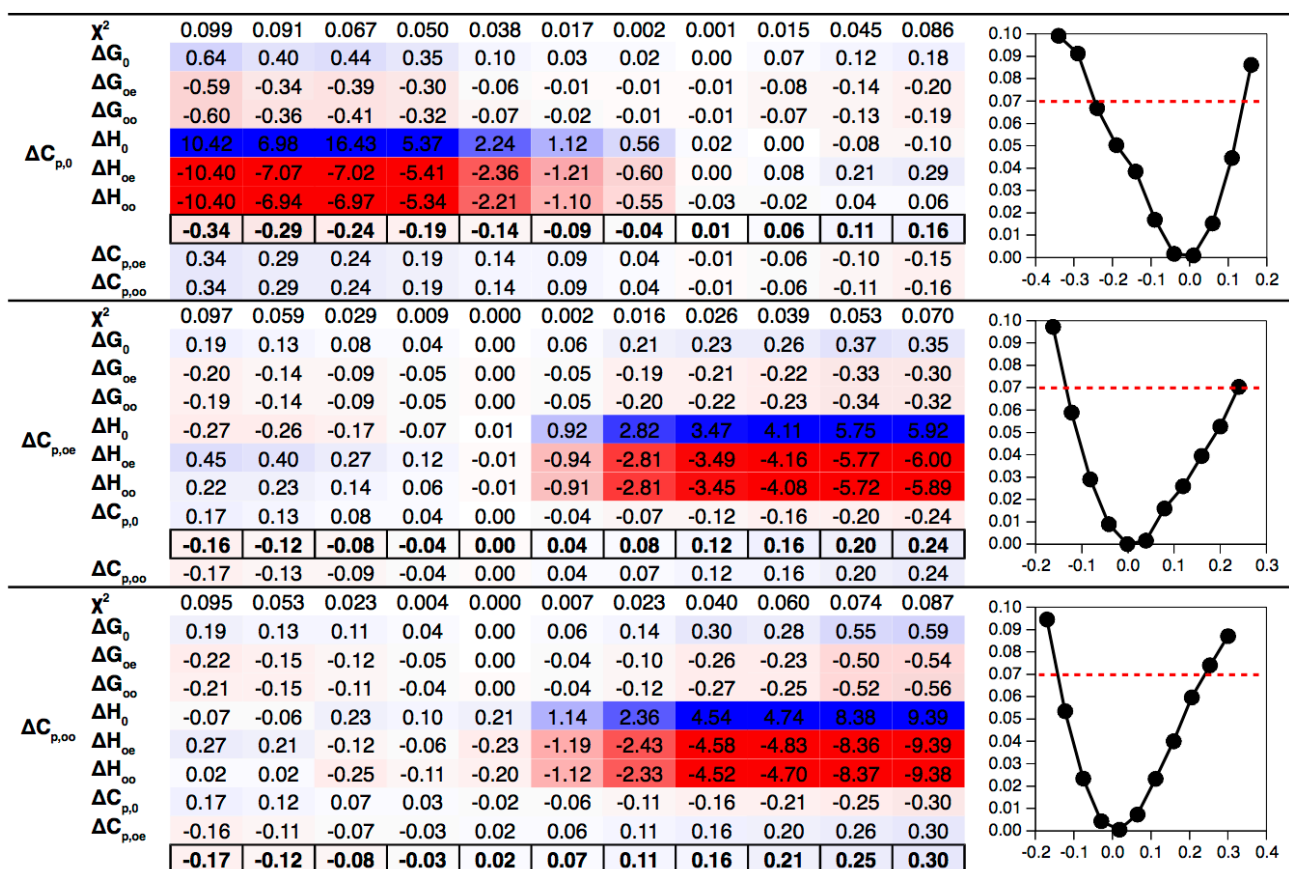
Supporting Figure 5. Best-fit thermodynamic parameters of binding to sites with zero, one, or two occupied neighbors, for model NN-na. ΔG , ΔH , and ΔS values are presented at the reference temperature of 40°C, ΔS is obtained through subtraction of independent ΔG and ΔH parameters. (A) Symmetrical error bars obtained from bootstrapping estimation with 200 replicates, parameters in the main text. (B) Asymmetrical error bars obtained from constant chi-square estimation, parameters from Table S2.



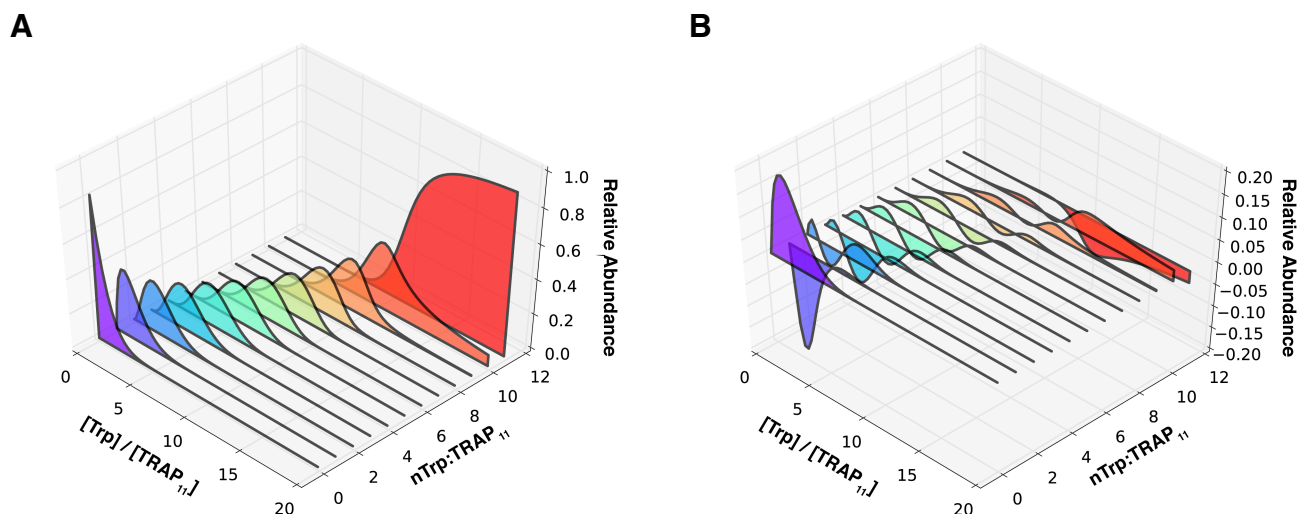
Supporting Figure 6. Chi-square error surfaces for the three ΔG parameters of model NN-na. To generate the one-dimensional error surfaces for ΔG_0 , ΔG_{oe} , or ΔG_{oo} , they are individually fixed to values in the outlined cells (shown here relative to the best-fit value, in kcal/mol), while the remaining model parameters are freely optimized. The final optimized value relative to the overall best-fit values for the remaining parameters are shown, and colored blue to red for positive or negative changes, respectively. The average χ^2 goodness-of-fit to experimental data deteriorates as the fixed parameter increases or decreases from its optimum value (graph on the right). The chi-square cutoff used to determine the ± 1 S.D. confidence interval is shown as a dashed red line.



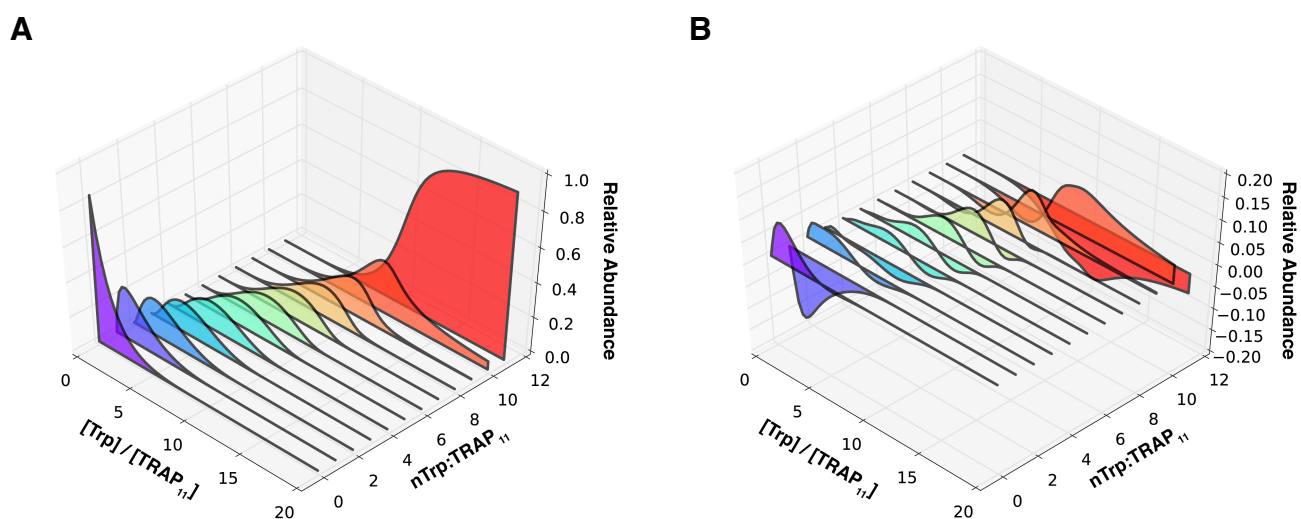
Supporting Figure 7. Chi-square error surfaces for the three ΔH parameters of the non-additive model NN-na. To generate the one-dimensional error surfaces for ΔH_0 , ΔH_{oe} , or ΔH_{oo} , they are individually fixed to values in the outlined cells (shown here relative to the best-fit value, in kcal/mol), while the remaining model parameters are freely optimized. The final optimized value relative to the overall best-fit values for the remaining parameters are shown, and colored blue to red for positive or negative changes, respectively. The average χ^2 goodness-of-fit to experimental data deteriorates as the fixed parameter increases or decreases from its optimum value (graph on the right). The chi-square cutoff used to determine the ± 1 S.D. confidence interval is shown as a dashed red line.



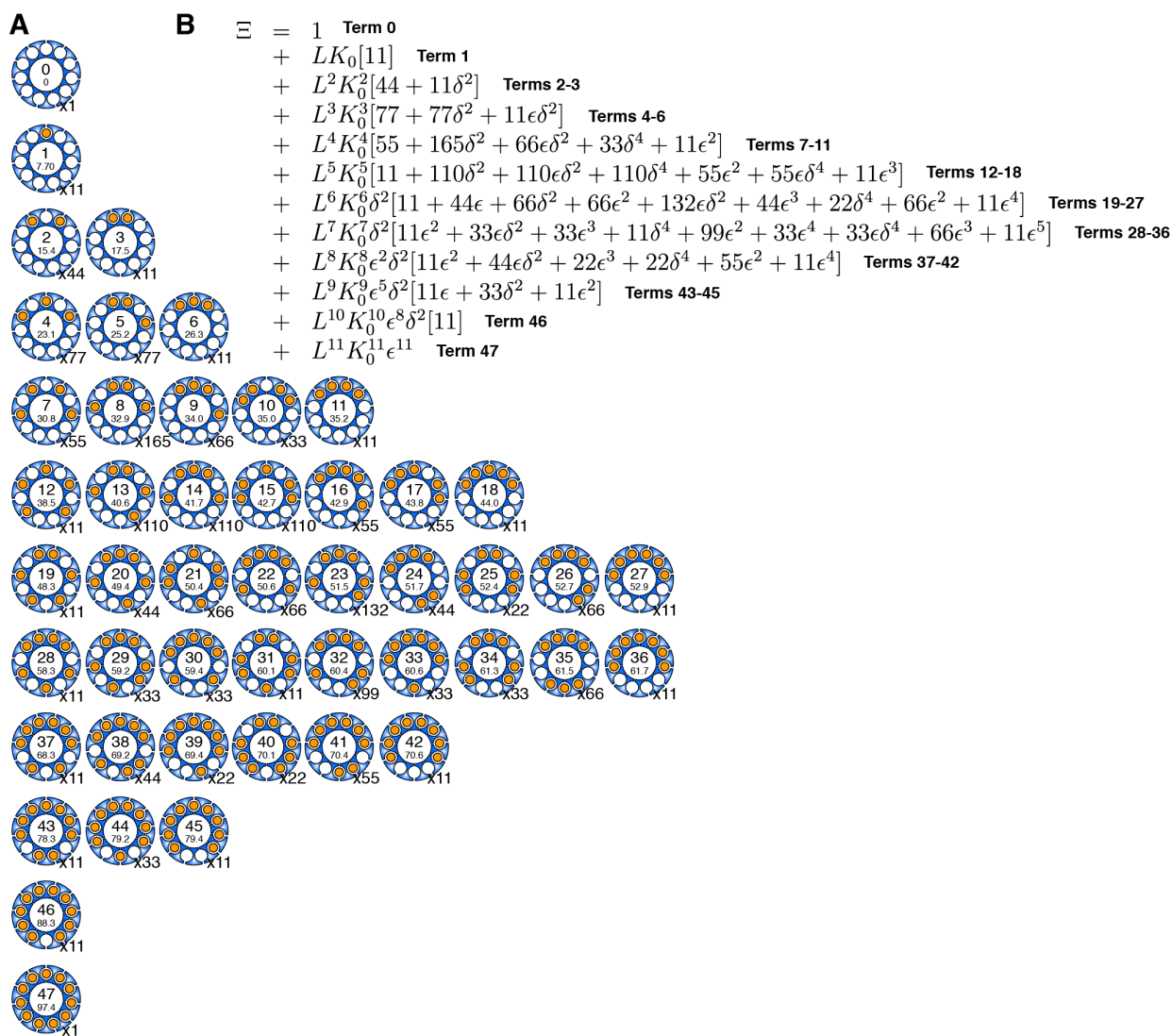
Supporting Figure 8. Chi-square error surfaces for the three ΔC_p parameters of model NN-na. To generate the one-dimensional error surfaces for $\Delta C_{p,0}$, $\Delta C_{p,oe}$, or $\Delta C_{p,oo}$, they are individually fixed to values in the outlined cells (shown here relative to the best-fit value, in kcal/mol·K), while the remaining model parameters are freely optimized. The final optimized value relative to the overall best-fit values for the remaining parameters are shown, and colored blue to red for positive or negative changes, respectively. The average χ^2 goodness-of-fit to experimental data deteriorates as the fixed parameter increases or decreases from its optimum value (graph on the right). The chi-square cutoff used to determine the ± 1 S.D. confidence interval is shown as a dashed red line.



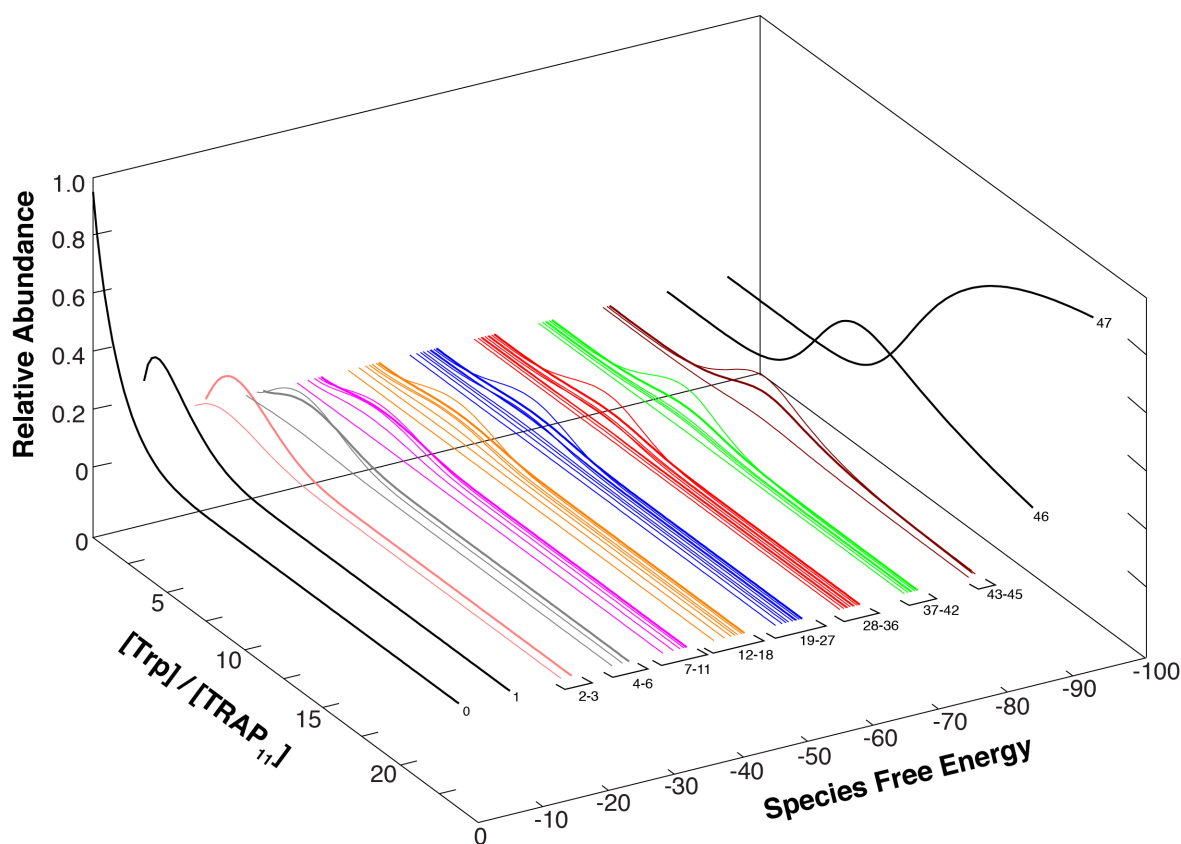
Supporting Figure 9. TRAP+nTrp populations for a non-cooperative binding model. (A) Relative abundance of the twelve TRAP+nTrp configurations present during the 40°C ITC titration at different Trp:TRAP ratios, using best-fit parameters for a non-cooperative model of eleven independent sites: ΔG : -9.31 kcal/mol (0.32 μ M K_d), ΔH : -17.93 kcal/mol, ΔC_p : -0.33 kcal/mol \cdot K. (B) The difference in populations predicted by a non-cooperative NN model and the non-additive NN-na model.



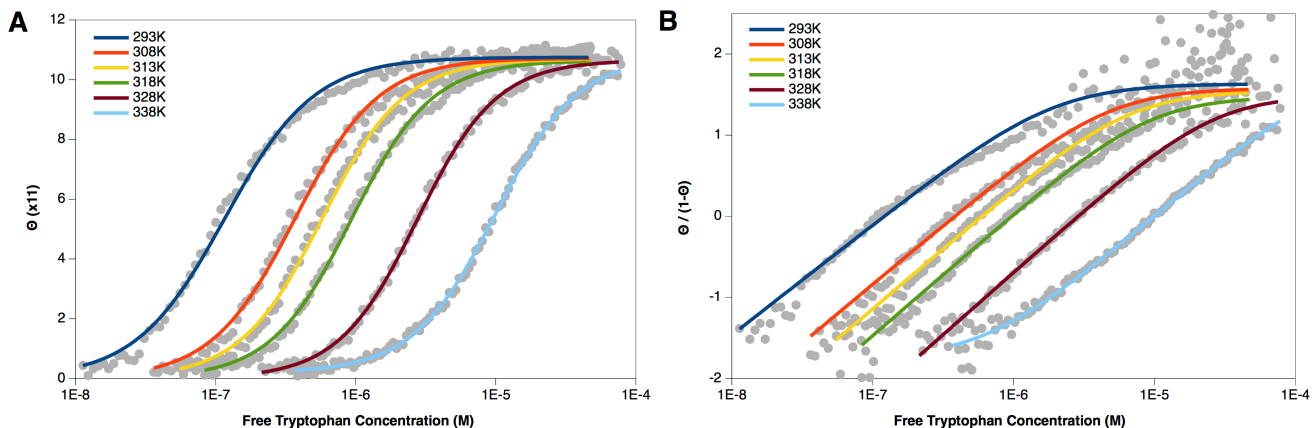
Supporting Figure 10. TRAP+nTrp populations for the additive NN-a model. (A) Relative abundance of the twelve TRAP+nTrp configurations present during the 40°C ITC titration at different Trp:TRAP ratios, using the best-fit parameters for model NN-a: ΔG_{bind} : -7.7 kcal/mol, $\Delta G_{\text{coupling}}$: -0.46 kcal/mol, ΔH_{bind} : -21.2 kcal/mol, $\Delta H_{\text{coupling}}$: 1.53 kcal/mol, $\Delta C_{p,\text{bind}}$: -0.40 kcal/mol \cdot K, $\Delta C_{p,\text{coupling}}$: 0.02 kcal/mol \cdot K. (B) The difference in predicted populations between models NN-a and NN-na.



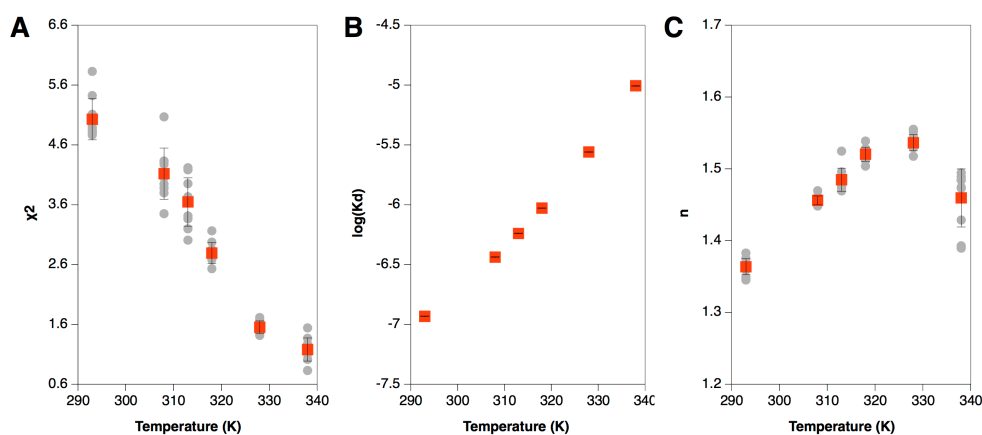
Supporting Figure 11. Representative TRAP+Trp configurations described in the non-additive nearest-neighbor model NN-na. (A) Diagrams of TRAP undecamers (blue) with 0-11 bound tryptophans (yellow), the multiplier on the bottom right of each configuration indicates the number of degenerate configurations sharing the same free energy. *Note that the diagrams for each distinct free energy are only representative, in that they may be just one of several different configurations of bound tryptophans possessing an identical energy.* Each representative configuration is numbered according to the term in the partition function in panel (B). Configurations are ordered left to right with decreasing (more negative / favorable) free energies, which are shown as smaller value below the configuration index number, in kcal/mol. These were obtained using the best-fit parameters values obtained from the experimental data, described in the article body.



Supporting Figure 12. Populations of energetically distinct TRAP+Trp configurations present during the 40°C ITC titration, using the best-fit parameters described in the main body for model NN-na. The relative abundances of the 48 energetically distinct TRAP+nTrp configurations described in figure S11 at each titration point are plotted in different colors. The lines for configurations are colored according to the number of Trp bound (e.g. pink = 2 bound tryptophans, gray = 3, magenta = 4, etc.) if there are different configurations possible, and are numbered to match the terms in Supporting Figure 4. The configuration with the largest negative free energy of each TRAP+nTrp stoichiometry are plotted with lines twice the thickness of the other configurations of the same stoichiometry. For TRAP states with between 4 to 9 bound tryptophans, configurations with second-largest negative free energy are actually most prevalent owing to their greater degeneracy.



Supporting Figure 13. Hill equation fits to TRAP₁₁ site occupancy predicted model NN-na, with added gaussian noise assuming 1% (SD) uncertainty in Θ . (A) Predicted site saturation as gray circles, over the experimental free tryptophan concentration ranges for the six sets of ITC data, fit using a 4-parameter logistic derivation of the Hill expression (colored lines). (B) Linearized Hill plot representation of the data shown in panel A.



Supporting Figure 14. Fitted Hill parameters of TRAP₁₁ site occupancy predicted by model NN-na. (A) Chi-square goodness-of-fit at each experimental temperature, gray circles are 10 different replicates generated using gaussian noise assuming 1% (SD) uncertainty in Θ . Orange squares are the mean value, with ± 1 SD error bars. (B) Fitted apparent Hill K_D at each experimental temperature. Symbols are same as panel A. (C) Fitted Hill n parameter at each experimental temperature. Symbols are same as panel A.